

# Modeling the Solvation of Peptides. The Case of (s)-N-Acetylproline Amide in Liquid Water

Chiara Cappelli\* and Benedetta Mennucci

Dipartimento di Chimica e Chimica Industriale, Università di Pisa, Via Risorgimento 35, I-56126 Pisa, Italy

Received: November 19, 2007; In Final Form: December 20, 2007

The structure and properties of (s)-N-acetylproline amide (NAP) in aqueous solution are studied by exploiting a continuum solvation model. The conformational preference of NAP as a function of the environment is discussed as well as data for a number of chiral and non-chiral spectroscopic and response properties (IR/VCD, Raman/VROA, UV/CD, ORD, NMR), whose calculation with the accounting of solvent effects is now possible due to recent developments introduced in the PCM approach. When available, calculated results are compared with experimental data, so as to evaluate the quality of the continuum approach to the solvation of this system.

## 1. Introduction

The study of solvation of proteins and peptides is an important issue in molecular biology and biochemistry.<sup>1</sup> Contrary to numerous experimental reports on the solvation of peptides and proteins and the large variety of theoretical studies on solvent-induced modifications of properties and reactivity of biomolecular systems, accurate quantum-mechanical (QM) studies on the nature of solvation of proteins are rather limited. This kind of study is in fact extremely complex, but such a complexity can be significantly reduced by utilizing the repetitive peptide group as the representative model system.

The simplest model for the amide linkage of peptides (and proteins) is *N*-methyl-acetamide, whose structure is considered as the basis for understanding the geometric constraints imposed by the peptide linkages that determine, at least partly, the protein structure and spectroscopic features.

The solvation of *N*-methyl-acetamide and its spectroscopic properties in the gas phase, in water and in acetone have been studied in two recent papers of our group<sup>2</sup> by exploiting a hierarchy of solvation approaches ranging from a purely continuum-only model to a supermolecule approach based on molecular dynamics (MD) simulations.

In this work, the problem of the modeling of the solvation of peptides is further addressed and applied to *N*-acetylproline amide in liquid water.

Various studies, both experimental and theoretical, have been addressed to the study of the secondary structure of dipeptides and in particular on the effect on it due to the surrounding environment. Most of such studies have focused on the alanine dipeptide, but an alternative system to investigate is *N*-acetylproline amide (NAP), where the free amine of a proline amino acid is blocked with an acetyl group, and the carboxyl group is replaced by an amide (Figure 1). *trans*-NAP (the most stable isomer, vide infra) can formally exist in various conformations, namely,  $\alpha$  helix,  $3_{10}$  helix I,  $3_{10}$  helix II,  $P_{II}$  and  $C_7$ , differing from each other by the values of the  $\phi$  and  $\psi$  angles (Figure 1). Previous studies, coupling molecular dynamics (MD) simulations with infrared (IR), Raman and vibrational circular dichroism (VCD) spectroscopies, have demonstrated that the

three-dimensional conformation of NAP strongly depends on solvent, particularly on the hydrogen-bonding ability of the solvent molecules, so that the predominant conformation in nonpolar solvent has been suggested to be the  $C_7$  structure. The conformation of NAP in polar, protic solvents, such as water or alcohols, is still controversial.<sup>3–5</sup> In particular, it has been recently demonstrated that the results obtained by using MD simulations strongly depend on the force field exploited, so that the ff03 force field of Amber8<sup>6</sup> predicts the polyproline-like  $P_{II}$  conformation to be the most stable in water, whereas a  $3_{10}$  helix conformation is found with ff99.<sup>3</sup> Also, the prediction of IR and vibrational circular dichroism (VCD) spectra of NAP made by coupling MD to the density functional theory (DFT) calculation of the appropriate vibrational tensors is dramatically different in the two cases, so that the comparison between calculated and experimental data shows the ff03 force field to be more reliable than ff99 in predicting the structure of NAP in water.<sup>3,5</sup>

Such findings show that care must be taken in using empirical force fields in the prediction of the secondary structure of peptides in solution.

Generally, in order to study the solvation of a complex system, such as a protein or a large peptide, either approximations in the description of intra- and intermolecular interactions or a reduction of the number of solvent molecules explicitly treated have to be done. The first case corresponds to classical simulations (Monte Carlo and MD), and the second case is the so-called supermolecule approach. The latter method has the notable feature of redefining the system to be accurately treated (usually quantum-mechanically) so as to include in the “solute” also a (small) number of solvent molecules, which should represent the first solvation shell(s). An alternative approach to these two is to use continuum solvation models (see, e.g., refs 7 and 8 and references therein). The potentiality of this approach, in which the molecular nature of the solvent is replaced by a structureless continuum description, is twofold: in fact, the dimension and the complexity of the problem remain almost unchanged with respect to the gas phase and at the same time such an approach is able to properly account for both polarization and long-range effects.

Also, modern continuum solvation models can be easily extended to include high-level QM descriptions and also

\* Corresponding author. Phone: +39-050-2219293. Fax: +39-050-2219260. E-mail: chiara@dcc.uniipi.it.

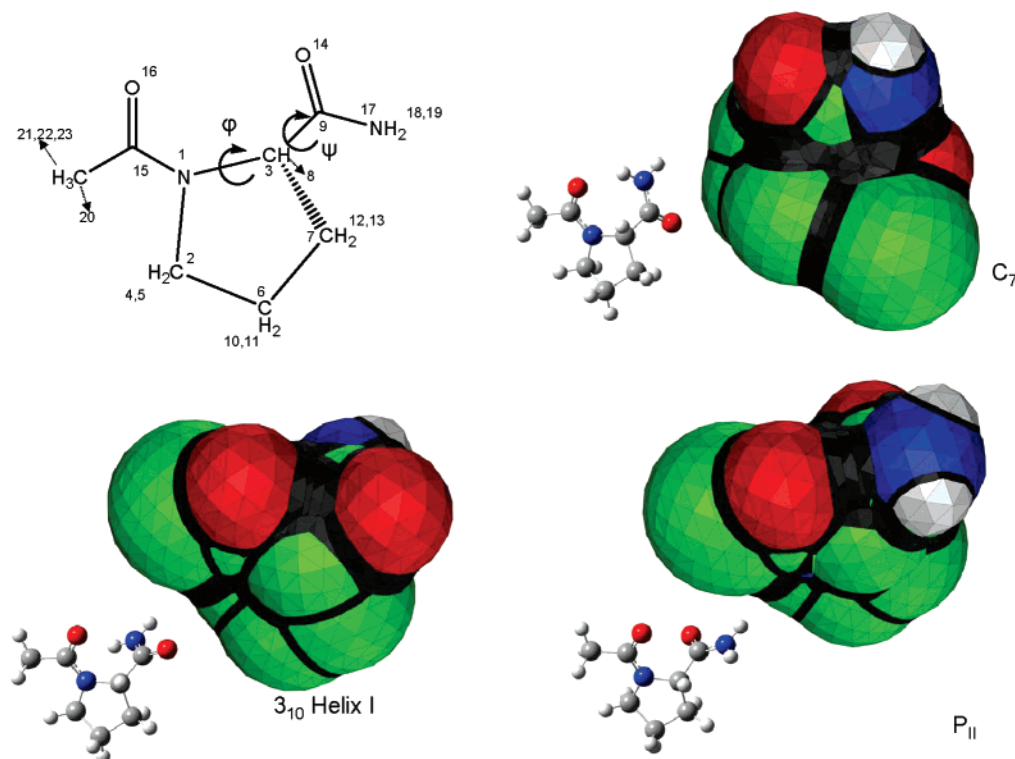


**Figure 1.** Schematic picture of NAP conformers with the indication of the  $\phi$  and  $\psi$  angles and the labeling of atoms. The PCM cavity is also shown.

generalized to compute various quantities such as equilibrium geometries and spectroscopic and response properties. Extensive literature on this topic can be found in recent reviews (see, e.g., refs 9 and 10). A notable feature of our solvation approach with respect to simulations is in fact that, while it is rather difficult (and sometimes not possible) to calculate molecular response properties from simulations, our approach can be in principle extended to treat any property with a given accuracy (i.e., to any QM level).

Continuum models, however, cannot completely describe an important part of solvation, namely, that related to local and/or specific interactions, for example, solute–solvent hydrogen bonding. To overcome such a limitation, continuum models can be coupled to supermolecule descriptions and/or to classical simulations. Such an approach has demonstrated to be very powerful in order to gain accurate description of systems and properties dominated by hydrogen-bonding effects (see, e.g., refs 9 and 11–13).

NAP can exist in trans and cis conformations, depending on the relative steric position of the acetyl group and the pyrrolidine ring. The potential energy barrier between the two isomers has been found to be relatively large, so that no conformational transitions between them can occur, and the time scale for such a conformational transition is slow enough to identify the two isomers in the NMR spectrum.<sup>3</sup> The spectroscopic properties of NAP have been experimentally studied by using a variety of techniques.<sup>3,5,14</sup> Focusing the attention to vibrational spectroscopies, among the various polypeptide vibrations, the amide I band has been known to be highly sensitive to the secondary structure of the peptide. In the case of NAP, two amide I local modes are detected in the spectrum, each involving the stretching vibration of one of the two carbonyl groups in the acetyl- and amide-end peptide bonds. Such two amide I frequencies have experimentally been found to be well separated from each other by about  $30\text{ cm}^{-1}$ . It has also been shown by Hahn et al.<sup>4</sup> by

exploiting MD that simulated IR and VCD spectra of the various conformations of NAP are greatly different from each other, thus showing that the overall averaged simulated spectra of NAP largely differ when one conformation or the other is predominant. Previous QM calculations on isolated NAP-like systems (such as Ac–Pro–NHMe and Ac–Pro–NMe<sub>2</sub>) have found the most stable conformations to be C<sub>7</sub>,<sup>15</sup> but the use of C<sub>7</sub> as the predominant conformation gives a wrong description of vibrational IR and VCD spectra in water solution.<sup>4</sup> Also, as it has been shown by Madison and Schellmann,<sup>14</sup> UV–vis, circular dichroism (CD) and optical rotatory dispersion (ORD) of NAP change dramatically if recorded in polar (water) or apolar (cyclohexane) solvents. Therefore, a key point in this field is certainly to get a reliable description of the conformational preference, on its dependence on the environment, and the evaluation of the spectroscopic properties with the account of the proper solvating environment.

In this paper, we will show how continuum solvation models constitute a valid alternative to MD simulations for the investigation of these issues of NAP. In particular, we will apply the continuum strategy to evaluate the conformational distribution and various spectroscopic properties—IR, Raman, VCD, vibrational raman optical activity (VROA), UV absorption and CD, ORD and NMR—of NAP in water solution. We will also compare our findings with both experiments and previous calculated MD data, so as to assess the quality of the continuum approach to such systems.

## 2. Computational Details

The structures of NAP stable conformations were optimized at the DFT level by using the B3LYP hybrid functional<sup>16</sup> and the 6-311++G(d,p) basis set both in vacuo and in water solution. Solvent effects were described by exploiting a continuum approach by means of the integral equation formal-

**TABLE 1: Dihedral Angle Values (in Degrees) for B3LYP/6-311++G(d,p) Optimized Structures in Vacuo (VAC) and in Water (WAT) (MD Data Taken from the Literature Are Also Reported)**

	$\phi$			$\psi$		
	VAC	WAT		VAC	WAT	
		PCM	MD <sup>a</sup>		PCM	MD <sup>a</sup>
$P_{II}$		-62	-78 (-69) <sup>b</sup>		146	149 (155) <sup>b</sup>
$3_{10}$ helix I	-76	-68	-71	-13	-28	-18 (-19) <sup>b</sup>
$C_7$	-81	-82	-81	77	74	71

<sup>a</sup> ff99,<sup>4</sup> <sup>b</sup> ff03.<sup>3</sup>

ism (IEF)<sup>17</sup> version of PCM (polarizable continuum model),<sup>18</sup> as implemented in the Gaussian 03 code (G03).<sup>19</sup> The molecular cavity surrounding the molecular solute was built by interlocking spheres centered on carbon, oxygen and nitrogen atoms (see Figure 1). The radius of each sphere was obtained by scaling the corresponding van der Waals radius by 1.2, thus obtaining  $R(C) = 2.04$  Å,  $R(CH) = 2.28$  Å,  $R(O) = 1.82$  Å and  $R(N) = 1.44$  Å.

Free energy gaps and Boltzmann populations in vacuo were obtained by including zero-point and thermal contributions. The same quantities in water were obtained in a similar way by further including nonelectrostatic (repulsion, dispersion and cavitation) energy contributions.<sup>9</sup>

IR, VCD and VROA spectra in solution were simulated by taking into account cavity field effects according to the model reported in ref 20. NMR nuclear shieldings were computed by using the Gauge-including atomic orbitals (GIAOs):<sup>21</sup> the inclusion of solvent effects within this formalism has been presented in ref 22. UV and CD spectra were obtained with the inclusion of solvent effects (see ref 9 for details). CD rotational strengths were calculated in the velocity gauge.

Specific rotations at 589 nm and a grid of selected wavelengths between 200 and 270 nm were calculated for each stable conformation in vacuo and water solution. Calculations were done according to ref 23, with further inclusion of cavity field effects.<sup>9</sup>

Raman and VROA spectra were obtained by numerically differentiating, with respect to the nuclear (normal) coordinates, the electric dipole–electric dipole, electric dipole–electric quadrupole and electric dipole–magnetic dipole polarizabilities (see refs 20a and 24 for details) obtained at a wavelength of 589 nm.

The reported IR, VCD, Raman and VROA spectra were drawn assuming Lorentzian line shapes (10 cm<sup>-1</sup> of half-width). The reported UV and CD spectra were obtained by summing averaged oscillator (rotational) strength weighted Gaussian curves with a full width of 0.15 eV at the 1/*e* of the maximum for each calculated electronic transition. ORD spectra were drawn by interpolating calculated OR averaged values on a grid.

### 3. Conformational Search

By following Hahn et al.,<sup>4</sup> five possible conformations of *trans*-NAP— $\alpha$  helix,  $3_{10}$  helix I,  $3_{10}$  helix II,  $P_{II}$  and  $C_7$ —were considered both as an isolated molecule and in water solution. Geometry optimization showed that only the  $3_{10}$  helix I and  $C_7$  are stable minima in the gas phase (Figure 1), whereas in water three structures, i.e.,  $3_{10}$  helix I,  $P_{II}$  and  $C_7$ , coexist. The conformational angles and the relative energies of the various optimized conformers are listed in Tables 1 and 2, respectively. At room temperature, in the gas phase, NAP assumes almost exclusively the  $C_7$  conformation, with only 1% of the  $3_{10}$  helix I. In water solution, the relative weights change, so that 68% is

**TABLE 2: Free Energy Gaps (in kcal/mol) at 298 K of Each Conformer with Respect to the Minimum Energy Structure Obtained after Full Optimization with B3LYP/6-311++G(d,p) in Vacuo (VAC) and Water (WAT) (The Normalized Boltzmann Factors (Bf) Are Also Shown; Nonelectrostatic Terms, Thermal and Zero-Point Contributions Are Included; MD Data Taken from the Literature Are Also Reported)**

	VAC		WAT		
	$\Delta G$	Bf	$\Delta G$	Bf	
				PCM	MD <sup>a</sup>
$P_{II}$			0.00	0.68	0.90
$3_{10}$ helix I	2.77	0.01	0.52	0.28	0.10
$C_7$	0.0	0.99	1.71	0.04	

<sup>a</sup> ff03.<sup>3</sup>

$P_{II}$ , 28% is  $3_{10}$  and  $C_7$  is about 4%. Such data are only partly in agreement with previous investigations based on MD calculations:<sup>3,4</sup> in fact, the Amber ff99 reported a prevalence of the  $3_{10}$  helix II conformer in water solution<sup>4</sup> ( $\phi = -74$ ,  $\psi = -4$ ), whereas further investigations with the ff03 force field demonstrated that the prevalent form of NAP in deuterated water is  $P_{II}$ , with a  $P_{II}/3_{10}$  helix I ratio of about 9 at room temperature.<sup>3</sup> Our calculations predict a net prevalence of  $P_{II}$  over  $3_{10}$  helix I (the  $3_{10}$  helix II is not a stable minimum) but a lower  $P_{II}/3_{10}$  helix I ratio, i.e., 2.4, with respect to the value given by MD simulations.<sup>3</sup>

Looking in detail to structural data, the  $3_{10}$  helix I structure is greatly influenced by the presence of the continuum environment: the  $\phi$  angle varies by about 10%, whereas  $\psi$  more than doubles (115% of increase moving from vacuo to water). On the other hand, the structure of the  $C_7$  conformer almost stays the same, showing only 1 and 4% variations of  $\phi$  and  $\psi$ , respectively. Such issues are not unexpected because in the  $3_{10}$  helix I both the two carbonyl groups and the  $-NH_2$  amino group are exposed to the solvent, and thus, the solvent can effectively interact with all three groups, which are all very hydrophilic (see molecular structures and sketches of the molecular cavities in Figure 1). On the other hand, inspection of the  $C_7$  structure shows features (bond distances and angles) compatible with the presence of an intramolecular O16–H19 hydrogen bonding: such an interaction can be seen as somehow “depleting” the solvent affinity of both the C=O and  $-NH_2$  groups, and thus, the least solvent dependent character of such a structure is understandable. Such findings, in combination with population weights (Table 2), are in agreement with what has been previously reported in the literature;<sup>5</sup> i.e., there is a competition for the acetyl-end carbonyl group between an intramolecular H-bonding and a solute–solvent interaction. When intramolecular H-bonding overtakes solute–solvent interaction, the  $C_7$  conformer is the dominating one, whereas, when intermolecular solute–solvent interactions dominate, the two other structures are more stable.

In order to better characterize the minima structures from the electronic point of view, in Table 3, molecular dipole moments and natural bond orbital (NBO) charges<sup>25</sup> of selected atoms are reported. Also, from an electronic point of view, the  $C_7$  structure is less solvent-sensitive than the  $3_{10}$  helix I: in fact, the changes both in the dipole moment and in the natural charges are always smaller for  $C_7$  than for  $3_{10}$  helix I moving from the gas phase to water; for instance, the dipole moment varies about 63% in the case of  $3_{10}$  helix I but only 28% in the case of  $C_7$ . Also, as expected, whereas in  $3_{10}$  helix I the two amino hydrogen atoms are almost equivalent, in the case of  $C_7$  one of them (H19) shows an enhanced charge, due to the fact that it is involved in



**TABLE 3: B3LYP/6-311++G(d,p) Molecular Dipole Moment (Debye) and Natural Charges (au) in Vacuo (VAC) and Water (WAT)**

	$3_{10}$ helix I		$C_7$		$P_{II}$
	VAC	WAT	VAC	WAT	WAT
	Dipole Moment				
	6.13	10.02	3.70	4.76	7.01
	NBO Charges				
O14	-0.62467	-0.72018	-0.63457	-0.70835	-0.71625
O16	-0.62832	-0.70908	-0.67821	-0.7322	-0.72012
N17	-0.80351	-0.78667	-0.80672	-0.79343	-0.78699
H18	0.3945	0.42293	0.38925	0.41564	0.42028
H19	0.3926	0.41761	0.42487	0.42899	0.42033

**TABLE 4: Vibrational Frequencies ( $\text{cm}^{-1}$ ) of Each Conformer (B3LYP/6-311++G(d,p) in Vacuo (VAC) and in Water (WAT); Experimental (exptl) and MD Calculated Data Are Also Reported)**

	VAC	WAT	MD
$P_{II}$		1642–1682	1613–1670, <sup>a</sup> 1580–1650 <sup>b</sup>
$3_{10}$ helix I	1717–1763	1650–1667	1629–1658, <sup>a</sup> 1580–1630 <sup>b</sup>
$C_7$	1683–1757	1632–1677	1593–1640 <sup>a</sup>
average	1683–1757	1643–1682	1585 <sup>a</sup> /1589 <sup>b</sup> –1635 <sup>a</sup> /1650 <sup>b</sup>
exptl <sup>b</sup>		1612–1650	

<sup>a</sup> ff99,<sup>4</sup> <sup>b</sup> ff03.<sup>3</sup>

intramolecular hydrogen bonding with O16. Such a charge difference between H18 and H19 in  $C_7$  is reduced roughly one-third going from vacuo to water, thus showing the reduced strength of the H-bond in water. H18 and H19 are equivalent in  $P_{II}$ , as expected. Paying attention to the two carbonyl oxygen atoms, i.e., O14 and O16, they are almost equivalent in  $P_{II}$  and  $3_{10}$  helix I (at least in the gas phase), whereas they have more variable charges in  $C_7$ . Once again, the reduction of the charge difference between O14 and O16 of  $C_7$  moving from vacuo to water shows that the O16–H19 H-bonding is stronger in vacuo.

A remarkable point is that the most populated conformer in water, i.e.,  $P_{II}$ , is not that with the highest dipole moment, being  $3_{10}$  helix I instead. Such a feature is particularly notable in the framework of continuum solvation approaches. In fact, simpler continuum models, such as the well-known Onsager model,<sup>26</sup> which models the solute in the solvent as a polarizable point dipole in a spherical cavity, would probably overestimate the conformational weight of  $3_{10}$  helix I with respect to IEFPCM, thus leading to averaged calculated properties differing remarkably from IEFPCM findings (vide infra).

Coming back to Table 2 and finally focusing on the comparison between calculated QM and MD populations, in general, the deviation between vacuo and MD is less than that between PCM and MD. Differences range from 1 to 36% in the case of PCM values and from 0 to 38% in the case of VAC data. Overall, taking the PCM values as reference, the MD data go toward the data in vacuo (VAC). One possible cause of this behavior can be that in the Amber ff003 force field solute–solvent mutual polarization effects are missed, which are instead accounted for in PCM.

#### 4. Vibrational Spectra: IR, VCD, Raman, and VROA

Calculated harmonic vibrational frequencies in the amide I range of the three relevant conformers in vacuo and water solution are reported in Table 4, together with MD results by Hahn et al.<sup>4</sup> and experimental findings by Lee et al.<sup>3</sup> As expected, DFT harmonic calculated values generally overestimate experimental data, but the calculated vs experimental scaling is quite different for vacuo and water, being about 0.95

(on average) and about 0.98, respectively. Thus, calculated data with the inclusion of solvent effects are decidedly in better agreement with experiments than the corresponding ones in vacuo. Going back to scaling factors, a whole set for B3LYP calculations in vacuo with a hierarchy of 6-311G-type basis sets has been reported by Andersson and Uvdal;<sup>27</sup> all factors shown there are in the range 0.96–0.97, thus showing apparently a lower agreement between our calculated and experimental frequencies. However, the set by Andersson and Uvdal is only composed of small gaseous molecules compared with experimental findings in the gas phase. To the best of our knowledge, the only reference for scaling factors of harmonic frequencies in solvent is a paper by our group,<sup>28</sup> which is however limited to ketones at the B3LYP/6-31G(d) level.

Looking again to Table 4, the comparison between our DFT values and MD ones<sup>3,4</sup> shows that the latter are generally lower. On average, MD values underestimate experimental values.

Focusing on the appearance of the whole vibrational spectra (frequencies and intensities), in Figure 2, calculated IR and VCD in the range 1500–1850  $\text{cm}^{-1}$  of the two relevant conformers ( $3_{10}$  and  $C_7$ ) in the gas phase are reported. The spectra are different depending on the conformation, both in frequency and in intensity: this is particularly relevant in the case of VCD, where the sign patterns are different if one conformer or the other is considered. Moving to aqueous solution, the presence of the solvating environment has a twofold influence on the solvated molecule: (a) the first effect on the molecule wavefunction and on the molecular PES (minima); (b) a second, indirect effect is that due to a change in the relative weights of the different conformers. In order to gain a detailed evaluation of solvent-induced effects, let us consider such effects separately.

The nature of the normal modes is not affected by the inclusion of the solvent: the three bands in the reported region of the IR spectrum can be assigned (from the lowest to the highest frequency) to an amide-II-type band of the terminal C–NH<sub>2</sub> group, an amide-I-type band mainly contributed by the C=O stretching mode of the C15–O16 carbonyl group and an amide-I-type band due to the C9–O14 carbonyl stretching mode. Such a band assignment is independent of the conformer, and is the same both in vacuo and in water solution. Although the normal mode nature does not change moving from vacuo to solvent, frequency and intensity values do. Looking in more detail to solvent effects causing such changes, it appears that the frequency shift in the amide I modes is strictly related to changes in the C=O bond distances. In fact, the highest frequency amide I mode, whose shift from vacuo to solvent is 95  $\text{cm}^{-1}$  for  $3_{10}$  and 80  $\text{cm}^{-1}$  for  $C_7$ , is accompanied by elongations of the related C9–O14 distances of about 0.02 Å ( $3_{10}$ ) and 0.01 Å ( $C_7$ ) going from vacuo to water for both conformers. Note also that such a difference in the C9–O14 carbonyl distance as a function of the environment is due to the fact that the C9–O14 carbonyl is conformationally exposed to the solvent; i.e., the solvent-induced geometrical change is in this case maximized.

Looking to averaged spectra (Figure 3), the inclusion of the continuum solvent around NAP with the consideration of solvent effects on the wavefunction and on the PES minima only (i.e., with populations calculated in vacuo) causes a large shift in the frequencies of the vibrational bands (about 100  $\text{cm}^{-1}$ ) and a completely different intensity pattern with respect to vacuo. Also, in the case of VCD, the inversion of the sign of the high-frequency amide I band at about 1775  $\text{cm}^{-1}$  in vacuo (1670  $\text{cm}^{-1}$  in water) is observed. The accounting of the large changes in the relative conformer populations in the two environments

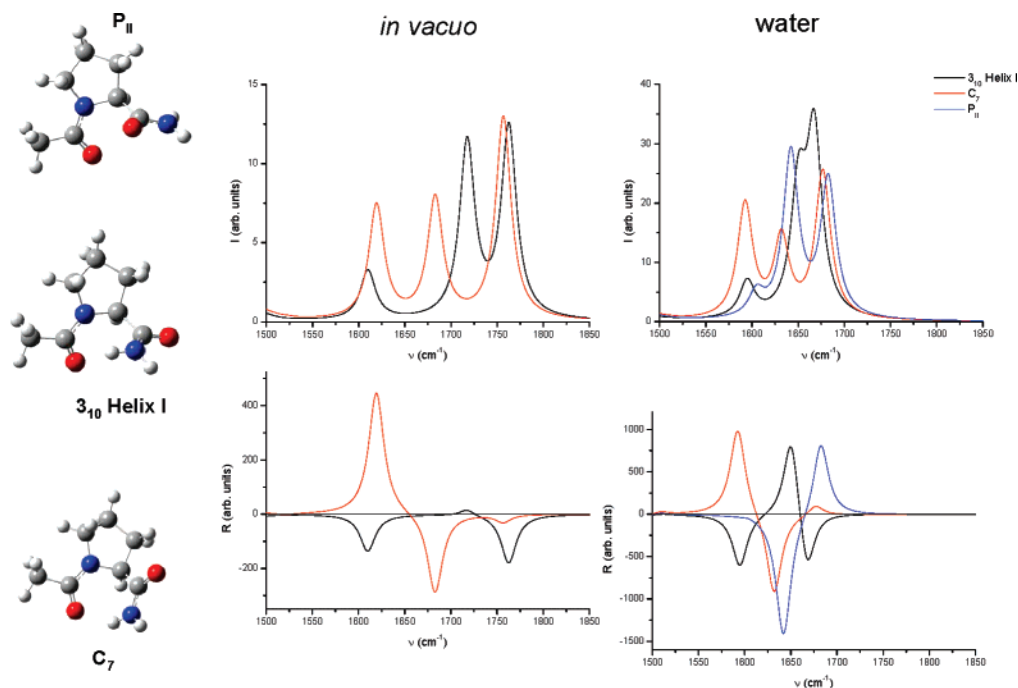


**Figure 2.** Calculated IR and VCD spectra for the various NAP conformers in vacuo and in water.

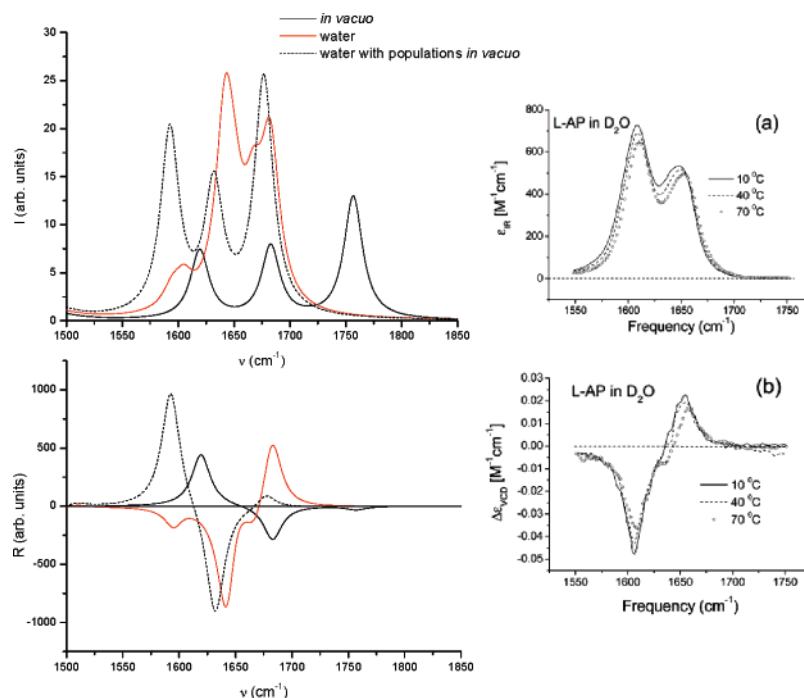


**Figure 3.** Calculated averaged IR and VCD spectra of NAP in vacuo, in water and in water with Boltzmann populations calculated in vacuo. Experimental spectra taken from ref 5 are also shown for comparison.

(vacuo and water) leads to completely different average IR and VCD spectra (see Figure 3, left). In fact, in the case of IR, an intense band with a totally different intensity pattern is observed. Differences are even more marked in the case of VCD, where a  $-/+$  rotational strength pattern is found by considering the total solvation effect, whereas roughly the opposite  $+/-$  alternation is found both in the gas phase and in the case of the sole consideration of solvent effects on the molecule wavefunction and PES minima.

Such findings can be compared with experimental IR and VCD spectra of NAP in  $D_2O$  reported by Oh et al.<sup>5</sup> (see Figure 3, right). Calculated data with the consideration of the total solvent effect are by far more accurate than the others in

reproducing the experiments. In particular, the double band in the IR is only reproduced by accounting for the whole solvent effect, whereas a totally different band structure is predicted both in the gas phase and with the discarding of solvent effects on conformer populations. Moving to VCD, the differences are even more dramatic, because the correct  $-/+$  pattern is reproduced only if the total solvation effect is taken into account, whereas a wrong spectrum is obtained in the other cases.

From the reported data, it can be concluded that the inclusion of “total” solvent-induced effects by means of continuum solvation approaches, i.e., in the calculation of the solute wavefunction, energy minima and conformational preferences, leads to a reliable description of the vibrational IR and VCD

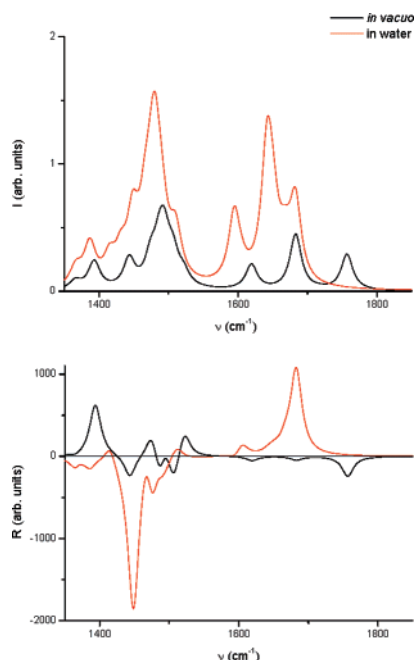


**Figure 4.** Calculated averaged Raman and VROA spectra of NAP in vacuo and water.

spectra of NAP. In light of the very good agreement between calculated and experimental data, it seems reasonable to assess that a purely electrostatic continuum model, i.e., a model not explicitly accounting for solute–solvent specific aggregation effects, such as hydrogen bonding, may model correctly the NAP–water interaction, at least as far as NAP vibrational properties are concerned. As a further comment on IR/VCD data, it should be noted that, due to the chemical nature of the NAP–water solvated system, it is natural to assess the presence of specific NAP–water hydrogen-bonding interactions. However, in the light of our results, it can reasonably be inferred that the accounting of such interactions in the computational model would modify the absolute values of the calculated properties (IR frequencies) probably tending toward the experimental results but not the overall picture described in Figure 3. In fact, looking again to Table 4, a discrepancy of about  $30\text{ cm}^{-1}$  is reported between our PCM data and experiments. Such differences should be reduced by introducing H-bond effects through a supermolecule approach (see, e.g., refs 2, 11 and 12). However, in our case, the main part of the solvent effects are due to solvent-induced conformational changes, and the relative weight of the three NAP conformers should not be largely changed by the inclusions of such effects: in fact, due to the geometrical conformation of the  $P_{II}$  and  $3_{10}$  structures, with the carbonyl groups well exposed to the solvent, it is reasonable to predict that such structures would be further stabilized against the  $C_7$  conformer by the accounting of specific interactions (for a discussion on this topic, see ref 29). Thus, as the overall appearance of the averaged spectra (Figure 3) is dominated by these two structures, no large differences are expected.

Still focusing on vibrational spectra, in Figure 4, averaged Raman and VROA spectra at 589 nm in the gas phase and in water solution are reported. The averaged Raman spectrum in water is more intense than the corresponding in vacuo spectra, and large differences in band relative intensities are reported. Moving to VROA, and similarly to VCD, a different intensity pattern is predicted as a function of the environment, both in band sign and relative intensities.

Looking more in detail to the reasons for such discrepancies, the same reasons reported above for IR/VCD also apply to

**TABLE 5: Absorption Maxima (nm) of Each Conformer B3LYP/6-311++G(d,p) in Vacuo (VAC) and Water (WAT)**

	VAC	WAT
$P_{II}$		190
$3_{10}$ helix I	202	193
$C_7$	203	196
average	203	191
exptl <sup>a</sup>		188

<sup>a</sup> Reference 14.

Raman/VROA. Calculated Raman/VROA spectra are very sensitive both to the molecular conformation and to the presence or absence of a solvating environment. On average, a marked difference in the spectra moving from a conformation to another and from gas to water is reported (spectra not shown, see the Supporting Information). In particular, focusing on spectra in the gas phase,  $C_7$  and  $3_{10}$  helix I show quite different Raman spectra but very dissimilar VROA spectra, with a completely different pattern both in sign but especially in relative intensities (see the Supporting Information). Thus, in this case, Raman and especially VROA appear to be powerful methods to characterize different conformers of the same molecule. In particular, VROA, which has been exploited so far only marginally in the study of conformational and response properties of molecular systems, appears once more a very powerful technique (see, e.g., ref 30), still deserving more interest. Moving to water solution, the same considerations just reported for the gas phase apply, with the additional feature of a very different behavior of the  $P_{II}$  conformer with respect to the other two, both in the case of Raman and VROA. We also note that in the dielectric continuum the sign of some of the VROA bands changes with respect to vacuo, e.g., the amide II band of  $C_7$  at about  $1600\text{ cm}^{-1}$ . Globally, Raman and VROA spectra appear to be very sensitive to the medium.

Such big differences in the spectra of the single conformers between vacuo to water turn out to be responsible for the different global appearance of the spectra averaged over the conformations (Figure 4). Unfortunately, to the best of our knowledge, neither Raman nor VROA spectra of NAP have been reported in the literature, so that we have no experiments to compare with our calculated data.

As a final comment of this subsection, we remark that all of our calculations rely on the double harmonic approximation; i.e., anharmonic effects have been neglected. Such an approximation surely introduces errors in the evaluation of frequency (and intensity/activity) values. As it has been shown by Wang and Hochstrasser,<sup>31</sup> the discrepancy between calculated harmonic and anharmonic amide I frequencies for *N*-methyl acetylproline amide in the gas phase is in the range  $30\text{--}50\text{ cm}^{-1}$ , i.e., of the order of our discrepancies between calculated and experimental values.

## 5. UV, CD, OR, and ORD

In this section, we report calculated data of electronic absorption and CD spectra, optical rotatory power and dispersion, which are among the most used techniques in the characterization of the chiral properties of peptides and peptide-like molecules: the comparison between calculated and experimental values will also be reported, when available.

In Table 5, absorption maxima (nm) of each conformer are reported: the values are almost the same in vacuo, whereas slightly different values are found in water, with a maximum deviation of 6 nm. The average value in water, 191 nm, compares pretty well with the experimental value of 188 nm as

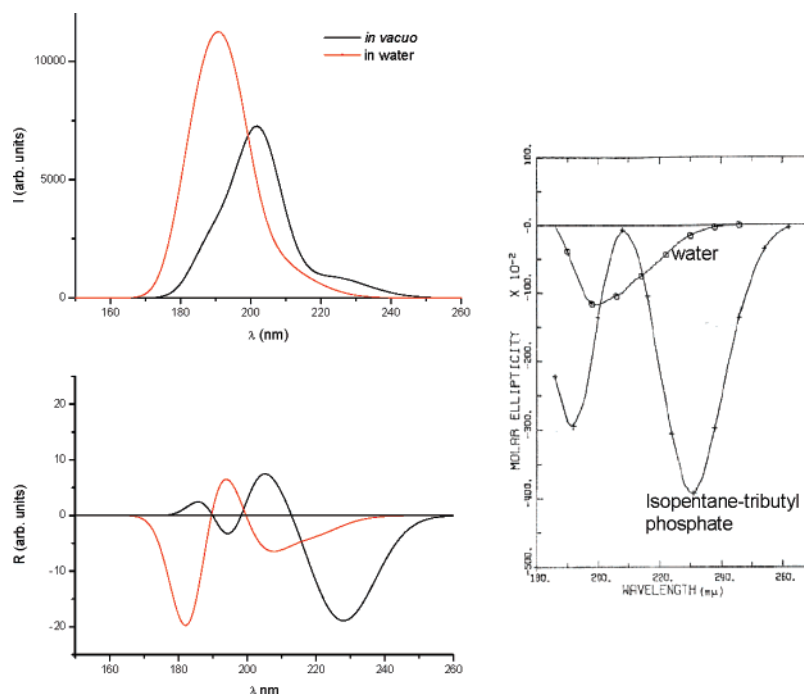


**Figure 5.** Calculated averaged UV and CD spectra of NAP in vacuo and water. Experimental CD spectra taken from ref 14 are also shown for comparison. (Reprinted with permission. Copyright 1970 John Wiley and Sons.)

**TABLE 6: Optical Rotation at 589 nm of Each Conformer B3LYP/6-311++G(d,p) in Vacuo (VAC) and Water (WAT)**

	VAC	WAT
$P_{II}$		−189
$3_{10}$ helix I	−186	−188
$C_7$	−215	−302
average	−215	−191

reported by Madison and Schellman;<sup>14</sup> the same does not occur for the averaged value in vacuo, which is 15 nm higher than experiments. Note that the wavelengths in Table 5 were obtained as the maxima of the simulated UV spectra for each conformer (see the Supporting Information). Such a choice is due to the fact that such broad bands result from contributions arising from a certain number (typically of the order of 5) of transitions of very similar character (i.e., involving a limited number of orbitals) very close to each other.

CD seems more suitable than UV for discriminating between conformers, yielding spectra which differ from each other not only in wavelength but especially in relative intensities of peaks (spectra not shown, see the Supporting Information). The sign of the bands and the +/− pattern is different moving a conformer to another, even if such differences are less marked than for VCD and VROA, independent of the environment.

Focusing on averaged spectra (Figure 5), CD in water appears quite dissimilar from the corresponding in vacuo. The calculated spectrum in water compares by far better than the one in vacuo with the experimental CD spectrum of NAP in water reported by Madison and Schellman<sup>14</sup> (see inset in Figure 5), whereas the spectrum calculated for the isolated molecule seems more similar to the experimental findings in apolar solvent, i.e., isopentane-tributyl phosphate: this is not surprising, in light of the low dielectric constant of such a solvent.

In order to investigate more on the chiral properties of NAP, calculated optical rotation (OR) at 589 nm in vacuo and in water are reported in Table 6. The same considerations already presented for CD also apply to OR. In particular, even if the sign of the calculated quantity does not change as a function of

the environment, both the OR values for the single conformers and the average value strongly depend on whether the solvent continuum is present or not. In particular, due to the strong variation in the OR value of  $C_7$  in combination with the large contribution of  $P_{II}$  in water, the average value decreases from −215 in the gas phase to −191 in water. To the best of our knowledge, no experimental OR values of NAP in water are reported in the literature, so that a direct comparison with experiments is not possible. Instead, averaged optical rotatory dispersion (ORD) curves of NAP in water and in apolar solvent (cyclohexane) have been reported by Madison and Schellman,<sup>14</sup> and therefore, plots of the calculated ORD curves obtained for the free molecule and in water solution are reported in Figure 6.

The difference between the two calculations is substantial, because a +/− pattern is predicted in vacuo, whereas a −/−, in water. With regard to the comparison with experiments (see inset in Figure 6), calculated and experimental data are in very good agreement, whereas the data in vacuo completely fail to reproduce the experimental sign in water. On the contrary, once again, calculations in vacuo compare well with the experimental data pattern in apolar solvent (cyclohexane), thus showing that the calculation of OR and ORD in vacuo can be considered a good approximation for reproducing data in apolar and non-protic solvents, whereas solute–solvent interactions must be properly modeled for reproducing such properties in polar solvents.

We finally note that, as it has been recently pointed out,<sup>32</sup> often the calculated electronic transition wavelengths do not match those observed experimentally. Then, the observed optical rotation data should not be compared to that calculated at the same wavelength, but such a comparison should be done at a wavelength that is shifted according to the difference between calculated and observed electronic transitions. In our case, however, due to the good agreement between experimental and calculated UV maxima of NAP in water (191 vs 188 nm), calculated wavelengths were not scaled.



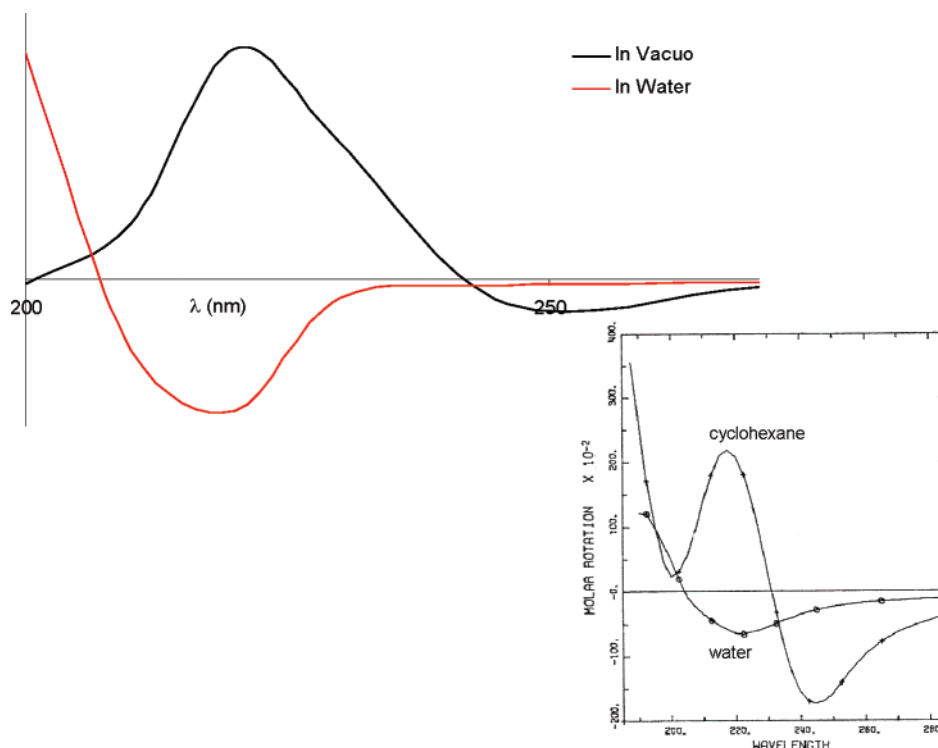


**Figure 6.** Calculated averaged ORD spectra of NAP in vacuo and water. Experimental ORD spectra taken from ref 14 are also shown for comparison. (Reprinted with permission. Copyright 1970 John Wiley and Sons.)

**TABLE 7: Averaged  $^1\text{H}$  Chemical Shifts with Respect to TMS (ppm) (B3LYP/6-311++G(d,p) in Vacuo (VAC) and Water (WAT))**

atom	VAC	WAT	exptl <sup>a</sup>
4	3.22	3.68	3.61–3.71 (m, 2H)
5	3.41	3.68	“ ”
8	4.51	4.44	4.38 (dd, 1H)
10	1.90	2.07	1.98–2.04 (m, 3H)
11	1.86	2.00	“ ”
12	1.79	1.97	“ ”
13	3.10	2.43	2.26–2.35 (m, 1H)
18	4.64	5.49	
19	7.70	6.07	
21	2.07	2.29	2.14 (s, 3H)
22	1.69	1.74	“ ”
23	1.97	2.15	“ ”

<sup>a</sup> In  $\text{D}_2\text{O}$ .<sup>3</sup>

## 6. NMR Spectra

Calculated average  $^1\text{H}$ ,  $^{13}\text{C}$ ,  $^{15}\text{N}$  and  $^{17}\text{O}$  NMR shieldings of NAP in vacuo and in water are reported in Tables 7 and 8:  $^1\text{H}$  and  $^{13}\text{C}$  are given as chemical shifts with respect to TMS.

Calculated  $^1\text{H}$  values in water are generally higher than the corresponding values in vacuo. The deviation between the two sets is in the range 1–22%. Overall, calculated values in water compare very well with experiments, and better than in vacuo data. Almost the same also applies to  $^{13}\text{C}$ , even if in this case the deviation between in vacuo and water results is less important. The correlation between calculated and experimental  $^{13}\text{C}$  chemical shifts is very good in both cases ( $R^2 = 0.9993$  in vacuo and 0.9998 in water), thus showing the account of the continuum environment to be less important to gain an accurate description of the carbon skeleton than to describe the proton shieldings.

Still referring to Table 8, calculated  $^{15}\text{N}$  and  $^{17}\text{O}$  NMR shieldings are also reported. The presence of the continuum around the molecule has little effect on the average  $^{15}\text{N}$

**TABLE 8: Averaged  $^{13}\text{C}$ ,  $^{15}\text{N}$  and  $^{17}\text{O}$  Nuclear Shieldings (ppm) ( $^{13}\text{C}$  Are Reported as Chemical Shifts with Respect to TMS; B3LYP/6-311++G(d,p) in Vacuo (VAC) and Water (WAT))**

atom	VAC	WAT	exptl <sup>a</sup>
2	52.69	54.04	51.5
3	62.54	66.97	62.71
6	28.48	30.15	27
7	30.28	36.23	32.94
9	175.65	183.94	180.21
15	175.26	178.33	176.04
20	25.17	25.43	24.24
N1	93.61	92.82	
N17	138.61	141.85	
O14	−70.38	−6.24	
O16	−78.21	−54.72	

<sup>a</sup> In  $\text{D}_2\text{O}$ .<sup>3</sup>

shieldings, leading to deviations with respect to vacuo of 0.8% for N1 and 2% for N17.

It is known that the most sensitive nuclei to the aqueous environment and to the local microenvironment are the oxygens. The data reported in Table 8 confirm these issues, showing a deviation on average values of about 30% for O16 and 91% for O14. Such big deviations are due to the differences in the calculated shieldings with or without the continuum solvent in combination with the relevant differences in the relative conformer populations. To investigate this point in more detail, in Table 9, calculated data for the various conformers are reported. Starting with O14 in vacuo, the two relevant conformers show quite similar  $^{17}\text{O}$  shieldings. This is not true with the inclusion of the continuum environment, which causes a net decrease in the absolute values (76% for  $3_{10}$  helix I and 61% for  $C_7$ ). Such a behavior is not unexpected, because the O14 atoms point outward from the molecular skeleton and thus they are in a similar molecular environment while being in the gas phase, but very exposed to the solvent in water solution (see



**TABLE 9:  $^{17}\text{O}$  Nuclear Shieldings (ppm) for the Various NAP Conformers (B3LYP/6-311++G(d,p) in Vacuo (VAC) and Water (WAT))**

	O14	
	VAC	WAT
$P_{\text{II}}$		−0.66
$3_{10}$ helix I	−74.17	−18.12
$C_7$	−70.07	−27.54

	O16	
	VAC	WAT
$P_{\text{II}}$		−51.93
$3_{10}$ helix I	−115.54	−62.43
$C_7$	−78.15	−45.70

**TABLE 10:  $^{17}\text{O}$  Nuclear Shieldings (ppm) for the Various NAP Conformers (B3LYP/6-311++G(d,p) in Vacuo (VAC), in Vacuo with Geometry Calculated in Water (VW), in Water with Geometry Calculated in Vacuo (WV) and Water (WAT))**

	VAC	VW	WV	WAT
$P_{\text{II}}$				
O14		−57.47		−0.66
O16		−108.34		−51.93
$3_{10}$ Helix I				
O14	−74.17	−84.39	−22.32	−18.12
O16	−115.54	−126.22	−62.40	−62.43
$C_7$				
O14	−70.07	−75.17	−27.57	−27.54
O16	−78.15	−80.49	−44.80	−45.70

Figure 1). For this reason, the solvent effect on the local electronic structure at O14 is the maximum in the series. As a further effect in solution, the shielding of  $P_{\text{II}}$  (which we recall is not a stable minimum in vacuo but is the dominant conformer in water) is very different from that of the two other conformations, due again to structural dissimilarity. On average, the combination of all of these effects (conformational weights plus direct solvent effects) leads to the net deviation (91%) for the calculated  $^{17}\text{O}$  shieldings going from vacuo to water solution.

Moving to O16, the calculated shieldings for  $3_{10}$  helix I and  $C_7$  are very different still in vacuo, and show a similar variation in percentage moving from vacuo to solvent (46 and 41%, respectively). In both cases, O16 is less exposed to the solvent than O14, but it is in a very different conformational framework: in fact, in the case of  $C_7$ , such a nucleus is involved in intramolecular hydrogen bonding with one of the H atoms of the  $\text{NH}_2$  group.

In order to better evaluate the large effect upon solvation on the predicted  $^{17}\text{O}$  shieldings, in Table 10, the effects due to changes in geometries and upon the inclusion of the continuum solvent are separately evaluated. By performing the calculation of the wavefunction and of the shielding with the inclusion of the continuum but with keeping the geometry fixed to the vacuum optimization (the WG column in Table 10), a 70% variation for  $3_{10}$  helix I and 61% for  $C_7$  in the case of O14 and 46–42% for O16 is observed, which in both cases causes a decrease in the absolute value. It is interesting to note that the calculation in vacuo with the geometry optimized in solvent (the GW column in Table 10) shows the opposite trend, i.e., leads to an increment in the shielding absolute values, whose entity is, however, by far less important, being in the range 0.1–13%, with the exception of O14 for  $3_{10}$  helix I, which further decreases about 16% with change of the geometry from vacuo to water. Again,  $P_{\text{II}}$  oxygens are the most solvent sensitive on average, showing a decrease in the values of about 99% (O14)

and 52% (O16) with the inclusion of the continuum solvent. In summary, from the analysis reported above, it seems that the inclusion of the continuum solvent around the molecule, i.e., the effect of the solvation of the wavefunction, is the most important one in determining the relevant changes in the  $^{17}\text{O}$  NMR shieldings, more than the solvent-induced changes in the geometry. Obviously, as already commented above, the very different values for the  $P_{\text{II}}$  conformer, in combination with its relevant conformational weight in water, lead to the big differences on the averaged values in vacuum and water. To the best of our knowledge, no  $^{17}\text{O}$  shielding measurements have been reported in the literature so far. In our opinion, however, our results show that the availability of such data would certainly shed light on the conformational preference of NAP in water.

## 7. Summary and Conclusions

In this paper, the structure and chiral and non-chiral spectroscopic and response properties—IR/VCD, Raman/VROA, UV/CD, ORD and NMR—of (*s*)-*N*-acetylproline amide in aqueous solution have been studied by exploiting the IEFPCM continuum solvation model.

The reported data, and the comparison with the available experimental data, have shown that the inclusion of solvent effects by means of a continuum solvation approach leads to a reliable description of NAP conformational and spectroscopic properties.

The explicit accounting of solute–solvent specific interactions, which are surely present in the NAP–water system, would probably modify the absolute values of the calculated properties but not the overall picture. In fact, as it has been shown, the main part of the solvent effects are in our case due to solvent-induced conformational changes: the relative weight of the three NAP conformers should not be largely changed by the inclusion of such effects; hence, no large differences are expected in the calculated properties.

The good performance of the continuum model may be commented in comparison with what has been previously reported in the literature with regard to a factor stabilizing the  $P_{\text{II}}$  conformer. In fact, it has been shown that the NAP structure in alcoholic solvents, which lack the possibility of making an extensive solvent-assisted H-bond network around NAP, is close to  $P_{\text{II}}$ ; i.e., a behavior similar to what was found in water was reported.<sup>5</sup> This can be a fundamental reason why our purely continuum approach succeeds in the evaluation of solvent effects on NAP: our model properly describes the electrostatic part of the H-bonding interaction, which seems to be the dominating term of such an interaction. On the contrary, the specific solvent networking around NAP, which leads to anisotropy in the solute–solvent interaction and eventually to solute–solvent charge transfer effects cannot be described by the IEFPCM in its basic formulation (for a discussion on this topic, see, e.g., ref 33): refinements in the approach would be necessary, such as the inclusion in the molecular system of some explicit solvent molecules around the solute. However, such an effect seems to be less relevant than the mean electrostatic effect in the case of NAP. Such a behavior obviously strongly depends on the peptide structure, and different results are expected as a function of the model chosen. However, the investigation of peptide structures and properties by means of the continuum solvation approach seems to be an interesting and promising research topic, which would warrant further closer investigation.

**Acknowledgment.** The authors thank Prof. Jacopo Tomasi for useful discussion and revision of the manuscript.

**Supporting Information Available:** Figures showing calculated Raman, VROA, UV and CD spectra of NAP conformers in vacuo and water. This material is available free of charge via the Internet at <http://pubs.acs.org>.

## References and Notes

- (1) Prabhu, N.; Sharp, K. *Chem. Rev.* **2006**, *106*, 1616–1623.
- (2) (a) Mennucci, B.; Martinez, J. *J. Phys. Chem. B* **2005**, *109*, 9818–9829. (b) Mennucci, B.; Martinez, J. *J. Phys. Chem. B* **2005**, *109*, 9830–9838.
- (3) Lee, K.-K.; Hahn, S.; Oh, K.-I.; Choi, J. S.; Joo, C.; Lee, H.; Han, H.; Cho, M. *J. Phys. Chem. B* **2006**, *110*, 18834–18843.
- (4) Hahn, S.; Lee, H.; Cho, M. *J. Chem. Phys.* **2004**, *121*, 1849–1865.
- (5) Oh, K.-I.; Han, J.; Lee, K.-K.; Hahn, S.; Han, H.; Cho, M. *J. Phys. Chem. B* **2006**, *110*, 13335–13365.
- (6) Case, D. A.; et al. *AMBER 8*; University of California, San Francisco: San Francisco, CA, 2004.
- (7) Roux, B.; Simonson, T. *Biophys. Chem.* **1999**, *78*, 1–20.
- (8) Orozco, M.; Luque, F. J. *Chem. Rev.* **2000**, *100*, 4197–4226.
- (9) Tomasi, J.; Mennucci, B.; Cammi, R. *Chem. Rev.* **2005**, *105*, 2999–3093.
- (10) Cramer, C. J.; Truhlar, D. G. *Chem. Rev.* **1999**, *99*, 2161–2200.
- (11) Cappelli, C.; Mennucci, B.; da Silva, C. O.; Tomasi, J. *J. Chem. Phys.* **2000**, *112*, 5382–5392.
- (12) Cappelli, C.; Mennucci, B.; Monti, S. *J. Phys. Chem. A* **2005**, *109*, 1933–1943.
- (13) (a) Mennucci, B. *J. Am. Chem. Soc.* **2002**, *124*, 1506–1515. (b) Cossi, M.; Crescenzi, O. *J. Chem. Phys.* **2003**, *118*, 8863–8872. (c) Aidas, K.; Møgelhøj, A.; Nielsen, H. K. C. B.; Mikkelsen, K. V.; Ruud, K.; Christiansen, O.; Kongsted, J. *J. Phys. Chem. A* **2007**, *111*, 4199–4210. (d) Kongsted, J.; Mennucci, B. *J. Phys. Chem. A* **2007**, *111*, 9890–9900.
- (14) Madison, V.; Schellman, J. *Biopolymers* **1970**, *9*, 511–567.
- (15) Kang, Y. K.; Park, H. S. *Biophys. Chem.* **2005**, *113*, 93–101.
- (16) Becke, A. D. *J. Chem. Phys.* **1993**, *98*, 5648–5652.
- (17) (a) Cancès, E.; Mennucci, B. *J. Math. Chem.* **1998**, *23*, 309–326. (b) Cancès, E.; Mennucci, B.; Tomasi, J. *J. Chem. Phys.* **1997**, *107*, 3032–3041. (c) Mennucci, B.; Cancès, E.; Tomasi, J. *J. Phys. Chem. B* **1997**, *101*, 10506–10517.
- (18) Miertus, S.; Scrocco, E.; Tomasi, J. *Chem. Phys.* **1981**, *55*, 117–129.
- (19) Frisch, M. J.; et al. *Gaussian 03*, revision B.05; Gaussian, Inc.: Wallingford, CT, 2004.
- (20) (a) Pecul, M.; Lamparska, E.; Frediani, L.; Cappelli, C.; Ruud, K. *J. Phys. Chem. A* **2006**, *110*, 2807–2815. (b) Cammi, R.; Cappelli, C.; Corni, S.; Tomasi, J. *J. Phys. Chem. A* **2000**, *104*, 9874–9879. (c) Cappelli, C.; Corni, S.; Mennucci, B.; Cammi, R.; Tomasi, J. *J. Phys. Chem. A* **2002**, *106*, 12331–12339. (d) Cappelli, C. In *Continuum Solvation Models in Chemical Physics: Theory and Applications*; Mennucci, B., Cammi, R., Eds.; Wiley: Chichester, U.K., 2007.
- (21) (a) Hammett, H. F. *Rev. Mod. Phys.* **1962**, *34*, 87–101. (b) Ditchfield, R. *Mol. Phys.* **1974**, *27*, 789–807. (c) Wolinski, K.; Hinton, J. F.; Pulay, P. *J. Am. Chem. Soc.* **1990**, *112*, 8251–8260.
- (22) (a) Cammi, R. *J. Chem. Phys.* **1998**, *109*, 3185–3196. (b) Cammi, R.; Mennucci, B.; Tomasi, J. *J. Chem. Phys.* **1999**, *110*, 7627–7638.
- (23) Mennucci, B.; Tomasi, J.; Cammi, R.; Cheeseman, J. R.; Frisch, M. J.; Devlin, F. J.; Gabriel, S.; Stephens, P. J. *J. Phys. Chem. A* **2002**, *106*, 6102–6113.
- (24) Corni, S.; Cappelli, C.; Cammi, R.; Tomasi, J. *J. Phys. Chem. A* **2001**, *105*, 8310–8316.
- (25) (a) Reed, A. E.; Weinhold, F. *J. Chem. Phys.* **1983**, *78*, 4066–4073. (b) Reed, A. E.; Weinstock, R. B.; Weinhold, F. *J. Chem. Phys.* **1985**, *83*, 735–746.
- (26) Onsager, L. *J. Am. Chem. Soc.* **1936**, *58*, 1486.
- (27) Andersson, M. P.; Uvdal, P. *J. Phys. Chem. A* **2005**, *109*, 2937–2941.
- (28) Cappelli, C.; da Silva, C. O.; Tomasi, J. *THEOCHEM* **2001**, *544*, 191–203.
- (29) da Silva, C. O.; Mennucci, B.; Vreven, T. *J. Org. Chem.* **2004**, *69*, 8161–8164.
- (30) (a) Hug, W. In *Handbook of Vibrational Spectroscopy*; Chalmers, J. M., Griffiths, P. R., Eds.; Wiley: Chichester, U.K., 2002. (b) Hug, W. In *Continuum Solvation Models in Chemical Physics: Theory and Applications*; Mennucci, B., Cammi, R., Eds.; Wiley: Chichester, U.K., 2007.
- (31) Wang, J.; Hochstrasser, R. M. *J. Phys. Chem. B* **2006**, *110*, 3798–3807.
- (32) Polavarapu, P. L. *Chirality* **2006**, *18*, 348–356.
- (33) (a) Tomasi, J.; Mennucci, B.; Cappelli, C. In *Handbook of Solvents*; Wypych, G., Ed.; ChemTec Publishing: 2000. (b) Alagona, G.; Ghio, C.; Cammi, R.; Tomasi, J. In *Molecules in Physics, Chemistry and Biology*; Maruani, J., Ed.; Kluwer: Dordrecht, The Netherlands, 1988.